

Transition to turbulence at the bottom of a solitary wave

Jan Pralits

Paolo Blondeaux & Giovanna Vittori

Dipartimento di Ingegneria Civile, Chimica e Ambientale - DICCA

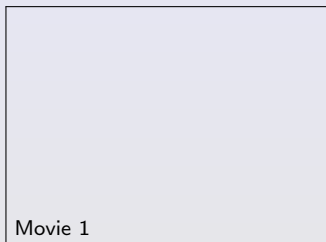
Università di Genova, Italia



Background

Far from the coast the influence of surface waves on the bottom layer is insignificant. As the waves move closer to the coast the shear stress in the boundary layer increases and destabilizes the upper layers of sediment. Even closer to the coast the boundary layer changes from laminar to turbulent and sediment transport increases.

For relatively small water depths, sea waves can be modeled as eg. **solitary waves**.



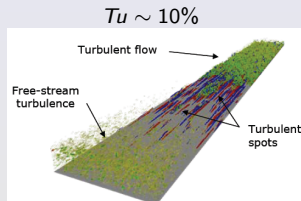
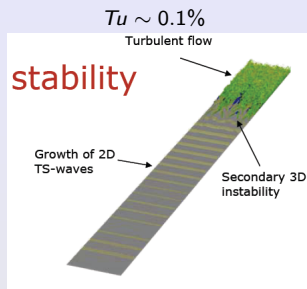
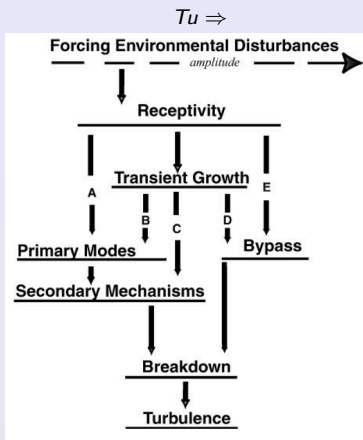
Exp. Sumer et al. (2010), JFM

The main differences between laminar and turbulent flow when it comes to sediment transport are

- Laminar flow : forces act locally on the sediment and the grain "diameter" becomes the important length scale
- Turbulent flow : large vortices "picks" up sediment, mixing, transport

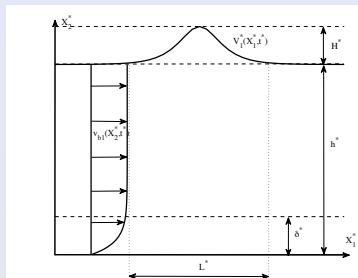
It is therefore of importance to understand in what circumstances (parametrically) the flow transitions

Routes to transition : complex & highly dependent on the surrounding conditions



Where do we start ? **Classical Modal analysis** Compare with DNS & Exp.

Definition of the basic flow : surface



Assume

$$H = H^*/h^* \ll 1$$

$$\mu = h^*/L^* \ll 1 \text{ (Boussinesq)}$$

with $H \sim \mu^2$, neglecting the wave damping and H^2 terms one obtains (Grimshaw, 1971) the free surface elevation and wave propagation velocity as

$$\eta^*(X_1^*, t^*) = H^* \operatorname{sech}^2 \left(\sqrt{\frac{3H}{4}} \zeta \right)$$

$$V_1^*(X_1^*, t^*) = H \sqrt{g^* h^*} \operatorname{sech}^2 \left(\sqrt{\frac{3H}{4}} \zeta \right)$$

where

$$\zeta = (X_1^* - \sqrt{g^* h^*} t^*)/h^* = X_1 - t$$

Note that:

$$U_{ref}^* = H \sqrt{g^* h^*} \quad L_{ref}^* = H^* \quad \text{and} \quad Re = U_{ref}^* L_{ref}^* / \nu^* = H \sqrt{g^* h^*} H^* / \nu^* \sim (H/\delta)^2$$

Definition of the basic flow : bottom boundary layer

The upper (air) boundary layer is neglected (τ_{xy} small)

In the bottom boundary layer viscous and inertial effects should balance

$$\frac{\partial}{\partial t^*} \sim \sqrt{g^* h^*} / h^*, \quad \nu^* \frac{\partial^2}{\partial X_2^{*2}} \sim \nu^* / \delta^{*2}$$

$$\rightarrow \delta^* \sim \sqrt{\nu^* h^* / \sqrt{g^* h^*}}$$

Here : $\delta^* / h^* \ll 1$, consequently we can use

Boundary Layer Approximation

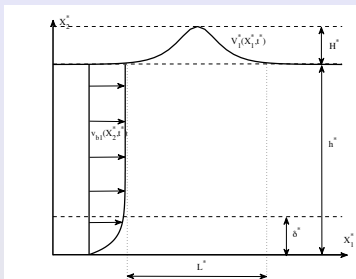
v_{b2}^* is negligible (continuity equation)

$\partial p^* / \partial X_2^* = 0$ (y momentum equation)

v_{b1}^* is then obtain by solving

$$\frac{\partial v_{b1}^*}{\partial t^*} = \frac{\partial V_1^*}{\partial t^*} \Big|_{X_2=0} + \nu^* \frac{\partial^2 v_{b1}^*}{\partial X_2^{*2}}$$

b.c : $v_{b1}^* = 0$ at $X_2^* = 0$ and $\frac{\partial v_{b1}^*}{\partial X_2^*} \rightarrow 0$ as $\rightarrow \infty$



$$Re_\delta = H \sqrt{g^* h^*} \delta^* / \nu^* = \sqrt{Re}$$

Definition of the basic flow : solution

Following Mei, "The applied dynamics of ocean surface waves" (1989), the solution can be written as

$$v_{b1}(X_2, \zeta) = \operatorname{sech}^2 \left(\sqrt{\frac{3H}{4}} \zeta \right) - \frac{2}{\sqrt{\pi}} \int_0^\infty \operatorname{sech}^2 \left[\sqrt{\frac{3H}{4}} \left(\frac{1}{2} \frac{X_2^2}{\xi^2} + \zeta \right) \right] e^{-\xi^2} d\xi, \quad \text{with } \zeta = X_1 - t$$

Case : Sumer et al. (2010), $H = 0.12$, $\delta = 0.0005$



Linear stability equations

We consider analyzing 2D perturbations and assume a decomposition as

$$(v_1, v_2, p) = (v_{b1}, 0, p_b) + \epsilon(v_{p1}, v_{p2}, p_p) \quad \text{where } \epsilon \ll 1,$$

and $U_{ref}^* = H\sqrt{g^*h^*}$, $L_{ref}^* = \delta^*$, $t_{ref}^* = L_{ref}^*/U_{ref}^*$, $p_{ref}^* = \rho^*Hg^*\delta^*$.

Linear stability equations

We consider analyzing 2D perturbations and assume a decomposition as

$$(v_1, v_2, p) = (v_{b1}, 0, p_b) + \epsilon(v_{p1}, v_{p2}, p_p) \quad \text{where } \epsilon \ll 1,$$

and $U_{ref}^* = H\sqrt{g^*h^*}$, $L_{ref}^* = \delta^*$, $t_{ref}^* = L_{ref}^*/U_{ref}^*$, $p_{ref}^* = \rho^*Hg^*\delta^*$.

We introduce the stream function: $v_{p1} = \partial\psi/\partial x_2$ and $v_{p2} = -\partial\psi/\partial x_1$.

Linear stability equations

We consider analyzing 2D perturbations and assume a decomposition as

$$(v_1, v_2, p) = (v_{b1}, 0, p_b) + \epsilon(v_{p1}, v_{p2}, p_p) \quad \text{where } \epsilon \ll 1,$$

and $U_{ref}^* = H\sqrt{g^*h^*}$, $L_{ref}^* = \delta^*$, $t_{ref}^* = L_{ref}^*/U_{ref}^*$, $p_{ref}^* = \rho^*Hg^*\delta^*$.

We introduce the stream function: $v_{p1} = \partial\psi/\partial x_2$ and $v_{p2} = -\partial\psi/\partial x_1$.

If we consider $H^* \gg \delta^* \Rightarrow H/\delta \gg 1$, then the perturbation amplitude grows on a time scale much faster than the basic flow.

Linear stability equations

We consider analyzing 2D perturbations and assume a decomposition as

$$(v_1, v_2, p) = (v_{b1}, 0, p_b) + \epsilon(v_{p1}, v_{p2}, p_p) \quad \text{where } \epsilon \ll 1,$$

and $U_{ref}^* = H\sqrt{g^*h^*}$, $L_{ref}^* = \delta^*$, $t_{ref}^* = L_{ref}^*/U_{ref}^*$, $p_{ref}^* = \rho^*Hg^*\delta^*$.

We introduce the stream function: $v_{p1} = \partial\psi/\partial x_2$ and $v_{p2} = -\partial\psi/\partial x_1$.

If we consider $H^* \gg \delta^* \Rightarrow H/\delta \gg 1$, then the perturbation amplitude grows on a time scale much faster than the basic flow.

The modal form of the stream function can therefore be written

$$\psi(x_1, x_2, t) = f(x_2, t) \exp \left[i\alpha \left(x_1 - \frac{H}{\delta} \int c(\tau) d\tau \right) \right],$$

Linear stability equations

We consider analyzing 2D perturbations and assume a decomposition as

$$(v_1, v_2, p) = (v_{b1}, 0, p_b) + \epsilon(v_{p1}, v_{p2}, p_p) \quad \text{where } \epsilon \ll 1,$$

and $U_{ref}^* = H\sqrt{g^*h^*}$, $L_{ref}^* = \delta^*$, $t_{ref}^* = L_{ref}^*/U_{ref}^*$, $p_{ref}^* = \rho^*Hg^*\delta^*$.

We introduce the stream function: $v_{p1} = \partial\psi/\partial x_2$ and $v_{p2} = -\partial\psi/\partial x_1$.

If we consider $H^* \gg \delta^* \Rightarrow H/\delta \gg 1$, then the perturbation amplitude grows on a time scale much faster than the basic flow.

The modal form of the stream function can therefore be written

$$\psi(x_1, x_2, t) = f(x_2, t) \exp \left[i\alpha \left(x_1 - \frac{H}{\delta} \int c(\tau) d\tau \right) \right],$$

and the governing equation at order ϵ becomes

$$[v_{b1}(x_2, t) - c(t)]\Delta f(x_2, t) - \frac{\partial^2 v_{b1}}{\partial x_2^2} f(x_2, t) = \frac{1}{2i\alpha(H/\delta)} \Delta^2 f(x_2, t),$$

Linear stability equations

We consider analyzing 2D perturbations and assume a decomposition as

$$(v_1, v_2, p) = (v_{b1}, 0, p_b) + \epsilon(v_{p1}, v_{p2}, p_p) \quad \text{where } \epsilon \ll 1,$$

and $U_{ref}^* = H\sqrt{g^*h^*}$, $L_{ref}^* = \delta^*$, $t_{ref}^* = L_{ref}^*/U_{ref}^*$, $p_{ref}^* = \rho^*Hg^*\delta^*$.

We introduce the stream function: $v_{p1} = \partial\psi/\partial x_2$ and $v_{p2} = -\partial\psi/\partial x_1$.

If we consider $H^* \gg \delta^* \Rightarrow H/\delta \gg 1$, then the perturbation amplitude grows on a time scale much faster than the basic flow.

The modal form of the stream function can therefore be written

$$\psi(x_1, x_2, t) = f(x_2, t) \exp \left[i\alpha \left(x_1 - \frac{H}{\delta} \int c(\tau) d\tau \right) \right],$$

and the governing equation at order ϵ becomes

$$[v_{b1}(x_2, t) - c(t)]\Delta f(x_2, t) - \frac{\partial^2 v_{b1}}{\partial x_2^2} f(x_2, t) = \frac{1}{2i\alpha(H/\delta)} \Delta^2 f(x_2, t),$$

This is an **eigenvalue problem** for the complex valued variable $c(t)$.

The so called dispersion relation can be written $c = c(H, \delta, \alpha, \zeta) = c_r + ic_i$.

c_r : phase speed, c_i : growth rate, $c_i > 0 \Rightarrow$ **unstable solution**.

Results

The results are presented in the following way

- Experiments by Sumer et al. (2010)*
 - U-shaped water tunnel excited by piston mechanism
 - $L \times H \times B = 10 \times 0.29 \times 0.39m^3$
 - Flow visualization with color CCD camera (25 frames/second)
 - shear stress (hot film probe) and free stream velocity (Laser doppler anemometer, LDA) measurements
- Linear Stability Analysis : critical conditions (ζ, α)
- Comparison with Direct Numerical Simulation

*Sumer et al. (2010), "Coherent structures in wave boundary layers. Part 2. Solitary motion", Journal of Fluid Mechanics, **646**, 207-231

Video (plan view) from Sumer et al. (2010)

Video from experiments by sumer et al. (2010)* where $H = 0.12$, $\delta = 0.0005$, flow from left to right. The video shows the vortex tubes in plan view.



*Sumer et al. (2010), "Coherent structures in wave boundary layers. Part 2. Solitary motion", Journal of Fluid Mechanics, **646**, 207-231

Video (side view) from Sumer et al. (2010)

Video from experiments by sumer et al. (2010)* where $H = 0.11$, $\delta = 0.00054$, flow from left to right. The video shows the vortex tubes in side view.

Movie 2



*Sumer et al. (2010), "Coherent structures in wave boundary layers. Part 2. Solitary motion", Journal of Fluid Mechanics, **646**, 207-231

Example result from LST: eigenfunctions

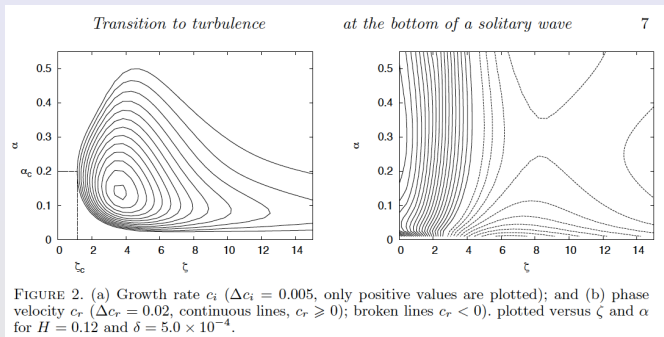
Case : Sumer et al. (2010), $H = 0.12$, $\delta = 0.0005$, $\alpha = 0.2$

Movie 1

Linear stability results

A worst case scenario can be assumed which requires to "scan" the whole parameter space, $\mathbf{c} = \mathbf{c}(H, \delta, \alpha, \zeta)$. In such a way critical conditions can be established as shown in the figure. Here it is shown that the instability occurs for $\zeta > 0$ which means the deceleration phase.

In this case $\zeta_c = 1.0$ and the corresponding wave number $\alpha_c = 0.2$.



Comparison with DNS

In Direct Numerical Simulations (DNS) the flow is computed without any approximations. It is therefore a "numerical experiment" to compare the Linear Stability (LST) results with. Two different DNS computations have been performed.

- Given initial condition of the perturbations
- Model of distributed wall roughness during the whole wave cycle

This gives different Receptivity scenarios and it is shown that the latter agrees better with LST (worst case scenario).

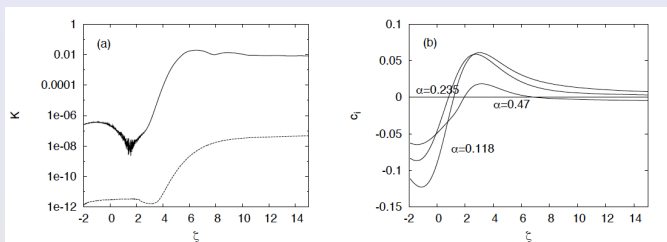


FIGURE 3. (a) Dimensionless kinetic energy per unit area K of the perturbations of the laminar boundary layer under a solitary wave, computed using the numerical approach of Vittori & Blondeaux (2008) for $H = 0.20$ and $\delta = 8 \times 10^{-4}$. The broken line is the value of K obtained introducing a perturbation of the laminar flow at the beginning of the numerical simulation and considering a perfectly plane wall, the continuous line is the value obtained introducing wall imperfections and considering vanishing initial condition. (b) Growth rate c_i plotted versus ζ for $H = 0.20$, $\delta = 8 \times 10^{-4}$ and three different values of α .

Summary of results : comparison between LST and experiments

Summary of experiments by Sumer et al. (2010) in comparison with Linear stability results. A reasonable agreement is found regarding the critical wave number α_c , while the critical time (LST) is under estimated.

Exp. no :	H	δ	α_c LST	α_c exp	ζ_c LST	ζ_c exp
1	0.12	0.0005	0.2	0.21-0.3	1.01	3.18
2	0.108	0.00054	0.2	0.23-0.3	1.16	4.77
3	0.199	0.00043	0.21	0.23-0.27	0.53	2.23
4	0.096	0.0006	0.205	0.19-0.26	1.39	4.81

Conclusions

- The solitary wave boundary layer is unstable if the height H exceeds a certain threshold, for a given boundary layer thickness δ .
- The instability sets in during the deceleration phase (for the parameters investigated).
- The critical wave length found by LST is similar to the distance between the vortex tubes found in the experiments by Sumer et al. (2010)
- The threshold wave height is under estimated by LST
- The discrepancy between DNS and LST might be explained considering different receptivity scenarios.

The work has been accepted for publication in the *Journal of Fluid Mechanics*